Proceedings from the University of Washington
School of Oceanography Senior Thesis, Academic Year 2012-2013

Air-sea CO_2 exchange in the Kuroshio and its importance to the global CO_2 uptake

Mitchell Chong[1]

[1]*University of Washington, School of Oceanography,*
Box 355351, Seattle, Washington 98195
mchong12@uw.edu
Received June 2013

NONTECHNICAL SUMMARY

The ocean is the largest sink of atmospheric CO_2. The Kuroshio Extension in the western North Pacific is a very significant region in the global CO_2 flux estimates. Measurements of surface concentrations of CO_2 during a 22-day cruise off the coast of Japan in the months of February and March 2013 were made to calculate the rate of CO_2 uptake by the Kuroshio Extension. Wind speeds were strongly correlated to the CO_2 flux and the axis of the current was found to have the highest rate of uptake. I estimated the area of the Kuroshio Extension and estimated the annual net uptake of carbon. This was compared to previous regional and global estimates to explore the importance of the Kuroshio Extension to the global CO_2 flux budget. Based on my estimates I conclude the Kuroshio plays a very significant role in the uptake of CO_2 in the North Pacific.

ABSTRACT

The Kuroshio in the western North Pacific is a region of high annual net CO_2 uptake. This large uptake of atmospheric CO_2 historically occurs during the winter months as low sea surface temperatures and high wind speeds increase the oceans uptake rate. Based on continuous sea surface temperature, sea surface salinity, wind speed, atmospheric pCO_2 and seawater pCO_2 data acquired from a cruise from February 25th to March 18th 2013, a spatial analysis of CO_2 flux in the Kuroshio Extension was examined. A northward and southward transect between 30°N and 40°N at 147°E was made to observe the atmospheric and surface water pCO_2 of the Kuroshio extention. The mean seawater pCO_2 across the extension was 343 ± 32 μatm and mean atmospheric pCO_2 was 396 ± 3 μatm. The mean ΔpCO_2 (-66 ± 11 μatm) indicates a net influx of carbon in the region. Mean wind speeds (10 ± 5 m s^{-1}) during the cruise had the largest effect on the CO_2 flux. The mean CO_2 flux during the cruise is estimated to be -11.9 mmoles CO_2 m^{-2} d^{-1}. By using annual measurements of pCO_2 at the Kuroshio Extension Observatory, I estimate the months per year the Kuroshio Extension is undersaturated in pCO_2. The area of the Kuroshio Extension is estimated to extend meridionally from 30°N to 40°N and longitudinally from 140°E to 160°W. I used the estimated area to calculate the net annual Carbon uptake of the Kuroshio (-0.14 Pg C yr^{-1}). Based on previous studies, the North Pacific accounts for 29% of the global oceans CO_2 uptake rate and this study further examines the significance of the Kuroshio Extension to the North Pacific CO_2 flux as well as the global CO_2 flux.

INTRODUCTION

Anthropogenic CO_2 has been altering the pre-industrial steady state conditions of the atmosphere for roughly 150 years. Recent time series data of atmospheric CO_2 at the Mauna Loa observatory has shown a rapid increase in concentrations over the past 50 years (Sarmiento and Gruber, 2002). The primary source of such accelerated concentrations of CO_2 is clear; anthropogenic inputs from fossil fuel burning has released more carbon into the system. The ocean is the largest sink of atmospheric CO_2 and it is important to understand the rate of carbon uptake in order to predict the impact of atmospheric CO_2 on the global carbon cycle, climate change and marine biogeochemistry.

The ocean has an estimated global annual net mean uptake of -2.22 Pg C yr^{-1} (Takahashi et al, 2002). One of the largest oceanic regions where atmospheric CO_2 is absorbed is the western North Pacific. In a North Pacific meridional band of 14°N to 50°N, the net annual air-sea CO_2 flux is estimated to be -0.64 Pg C yr^{-1}. Of the global 2.22 Pg C yr^{-1}, the North Pacific is responsible for 28.9% of the net annual global ocean uptake of CO_2. The Kuroshio is a Western Boundary Current converging with the southward flowing Oyashio. SSH anomalies created by the subtropical waters transported by the Kuroshio and the subtropical waters transported by the Oyashio create strong eastward geostrophic flow in the Kuroshio Extension. The region is characterized and associated with strong geostrophic flow, SST anomalies, and eddies. (Cheney, 1977). The Kuroshio Extension, a meridional band of 30°N to 40°N is one of the strongest sinks of atmospheric CO_2 (Takahashi et al., 2002). The net flux of the Kuroshio Extension is estimated to be between 0.14 and 0.36 Pg C m^{-2} yr^{-1} (Takahashi et al, 2002). This estimate is approximately half of the North Pacific flux estimate. Kuroshio seawater pCO_2 is increasing at 1.5 μatm yr^{-1} (Murata et al., 1998) therefore it is also important to understand the influences of carbon uptake in the region.

There are two significant influences on the air-sea CO_2 flux, wind speed and the solubility of gas in seawater. Gas transfer rates increases with the square of the wind speed (Wanninkhof, 1992). There is a positive relationship between gas solubility in seawater and flux rates. The solubility of gas in seawater is dependent on temperature and salinity (Weiss, 1974). The Kuroshio Extension is characterized by the convergence of warm subtropical waters from the equator and cold subarctic waters from the north. The resulting eastward current is geostrophic advection due to a large SSH gradient at the axis of the current (Qiu, 2002). The geostrophic advection at the axis results in heat transport away from the region and low SST (Qui and Chen, 2005). Eastward geostrophic advection of the Kuroshio Extension also transports dissolved inorganic carbon (DIC) surface water away from the region. The resulting low DIC water allows the influx into the region because pCO_2 has also decreased (Ayers and Lozier, 2012). The combination of strong winds, convergence of sub-arctic and sub-tropical waters, and strong geostrophic advection makes the Kuroshio Extension a region of high CO_2 uptake.

The Kuroshio Extension Observatory (KEO) mooring has provided continuous SST, SSS and pCO_2 measurements since 2004 (Cronin et al., 2008). Temporal variability of pCO_2 at KEO has been observed and measurements of pCO_2 from KEO show an annual undersaturation between the months of October and July. The Kuroshio extension is characterized by high CO_2 uptake (Cronin et al., 2008) and pCO_2 annual undersaturaion. During the seasonal maximum udersaturation, February 2010, mean seawater pCO_2 was -57 ± 3 μatm. (Data provided by NOAA-Pacific Marine Environment Laboratory, Kuroshio Extension Observatory; Seattle, Washington; website: http://www.pmel.noaa.gov/keo/).

Few studies have estimated the annual CO_2 flux of the Kuroshio extension but rather the North Pacific basin. Inoue et al. (2002) examined the distribution of pCO_2 in the Kuroshio Extension between Japan and the Hawaiian Islands but did not estimate the CO_2 flux. This study will examine the spatial variability of the Kuroshio extension while integrating the temporal variability of the KEO to estimate the regional uptake of CO_2. With the high-resolution spatial variability observed from the cruise, an estimation of the Kuroshio's significance to the regional CO_2 uptake is made and compared to previous estimates.

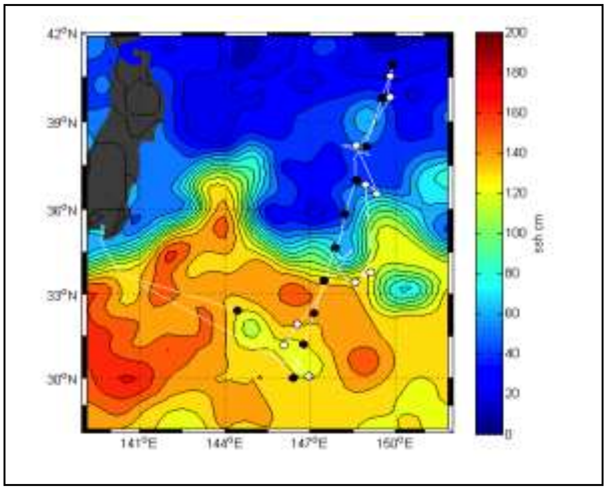

Fig. 1 Satellite SSH map of the Kuroshio Extension and the cruise transect. Courtesy of Byron Kilborne.

METHODS

A 22 day cruise aboard the *R/V Melville* departing from Yokohama, Japan made a transect from 30°N to 40°N, returning to 30N along a 147°E to 148°E longitudinal band (fig. 1). Data were collected from March 1st, 2013 to March 16th, 2013. During the first four days of the cruise, the pCO_2 system was not recording data therefore data from latitudes between 30°N and 34°N were obtained during the northward transect of the cruise. Continuous measurements were made during the remainder of the cruise at latitudes between 30°N and 41°N. Continuous atmospheric pCO_2 and seawater pCO_2 was measured with an automated underway system provided by the NOAA Pacific Marine Environment Laboratory. NOAA PMEL also provided instrument installation and processed pCO_2 data. Uncontaminated seawater is pumped into the analyzer through a ship's seawater intake system. Air in the analyzer is equilibrated with the seawater and measured approximately every 10 minutes. Atmospheric pCO_2 is measured three times an hour with a separate supply airline from the bow of the ship. CO_2 measurements are made using a non-dispersive infrared analyzer and calibrations are made each hour using three CO_2 standards (Feely et al., 1998). Sea surface temperature, sea surface salinity and wind speed were recorded using the *R/V Melville* MET data systems.

The CO_2 flux was calculated using the wind driven gas transfer velocity of CO_2, the solubility of CO_2 in seawater and the difference of pCO_2 between the ocean and the atmosphere.

1. $F = k * S * \Delta pCO_{2\ sw\text{-}atm}$

The flux (F) is determined by multiplying the mass transfer coefficient (k) by the gas solubility in seawater (S) by the difference in pCO_2 ($\Delta pCO_{2\ sw\text{-}atm}$).

2. $\Delta pCO_2 = [pCO_2]^{sw} - [pCO_2]^{atm}$

3. $k = (0.222*U^2 + 0.333U)(Sc/600)^{-1/2}$ cm hr^{-1}

4. $Sc= \nu/D_c$

The pCO_2 (μatm) is the partial pressure of CO_2 in the atmosphere or seawater. The ΔpCO_2 is calculated using the measurements of seawater and atmospheric pCO_2 measured by the underway system provided by NOAA PMEL. The ΔpCO_2 is the difference in CO_2 partial pressures (seawater-atmosphere) and its sign determines the direction of gas diffusion. A negative ΔpCO_2 indicates influx of gas into the ocean. The k (m d^{-1}) term of the flux equation is the air/water exchange mass transfer coefficient, which is dependent on wind speed U (m s^{-1}) and the Schmidt number (Sc). The Schmidt number describes the ratio of the kinematic viscosity (ν) of seawater to its molecular diffusivity (D_c) and is dependent on the temperature and salinity of seawater (Emerson and Hedges, 2008). Each pCO_2 measurement, k was normalized to Schmidt number of 600 (Wanninkohf, 1992; Nightningale et al, 2000). Wind Speed (U) is measured in m s^{-1} by the shipboard meteorological systems. The gas solubility term (S) in the flux equation is calculated from SST and SSS and is reported in mol m^{-3} atm^{-1} (Weiss, 1974). The resulting air-sea exchange rate (F) is expressed in mmol C m^{-2} d^{-1}.

RESULTS

I estimated the meridional boundaries based on SSH anomalies (fig. 1) however a T-S analysis (fig. 2) confirmed the mesoscale boundaries of the Kuroshio Extension. The meridional boundaries of the Kuroshio Extension was determined to be latitudes between 30°N and 38°N with the axis of the current between 34°N and 38°N and latitudes north of 38°N is subarctic water masses. In Fig. 2 regions are defined by isopycnals. The variability in densities at the current axis is due to a large SST gradient between 36°N and 38°N (Fig. 3).

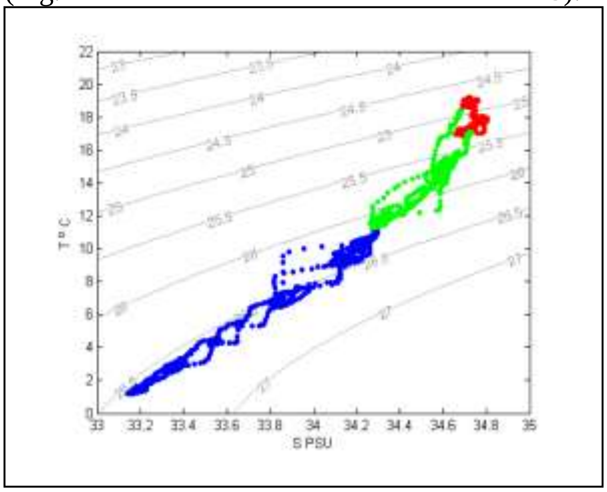

Fig. 2. T-S plot of SSS and SST during the cruise prior to errors in MET data at 40°N. The blue region indicates the Kuroshio extension south of the current axis. The red region indicates the current axis and the green region indicates the northern boundary of the Kuroshio extension. Courtesy of Hilary Palevsky

The sub arctic region is all latitudes north of 38°N. The SST at 40°N decreased precipitously, indicating another water boundary. The blue data in fig.2 is near the σ_θ=26.5 isopycnal supports the SST observations. Mean SST and SSS in the subarctic region was 7.5°C ± 4.0 and 33.89 ± 0.47 per mille, respectively. The axis of the Kuroshio Extension is between 34°N and 38°N. A large SSH gradient is observed between these latitudes (fig. 1). Figure 3 also shows the large SST gradient between 36°N and 38°N. Variability in SST (15.2°C ± 1.9) were due to mesoscale features in this meridional band. Satellite SSH data supports the SST observations with multiple SSH contours ranging from approximately 20 cm to 130 cm (fig.1). The axis is represented as green in fig.2 where densities are more variable than the sub arctic waters. Mean SST and SSS at the axis were 15.2°C ± 1.9 and 34.46 ± 0.23 per mille, respectively. The non-axis region of the Kuroshio is between 30°N and 34°N. I believe the northern front of subtropical waters did not extend north of 30°N. SST data does not indicate a clear boundary of increased SST, which would indicate presence of subtropical waters. Mean SST and SSS in this region was 17.5°C ± 0.36 and 34.80 ± 0.22 per mille, respectively.

Sea surface salinity is an accurate seawater property to evaluate when defining water mass boundaries however problems with the shipboard thermosalinograph produced errant data starting March 6th 2013 for the remainder of the cruise. Discrete samples of salinity were collected every 2-4 hours thereafter and were used to calibrate the shipboard thermosalinograph. SSS is necessary for calculating the gas solubility in seawater term (*S*) in the flux equation however it is not the dominating factor in the solubility CO_2 in seawater. The Kuroshio Extension is variable in its SSS properties and the mean SSS across latitudes 30°N to 41°N was 34.42 ± 0.4 per mille.

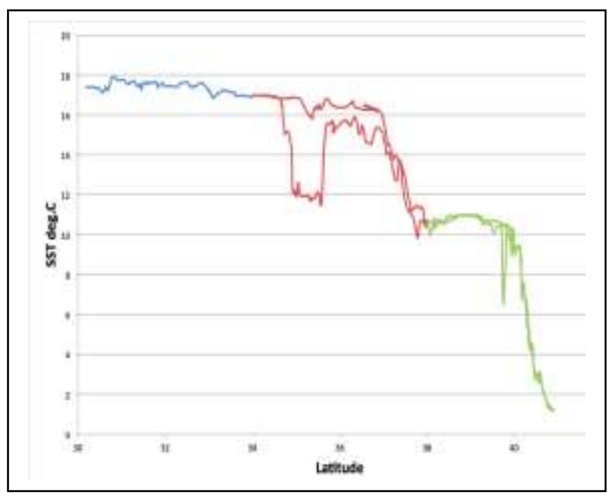

Fig. 3. Observed SST at latitudes between 30N and 41N. The blue region indicates the Kuroshio Extension south of the current axis. The red region indicates the current axis and the green region indicates the northern boundary of

the Kuroshio Extension. Differences in SST at like latitudes is due to differences during northward and southward transects. Rapid changes in SST as well as SSH (Fig. 1) were used to determine the mesoscale boundaries of the Kuroshio extension.

Over 4500 data points of seawater and atmospheric pCO_2 were collected during the cruise. Latitudes between 30°N and 41°N were measured for pCO_2 and mean seawater concentrations was 343 ± 32 µatm. Mean atmospheric pCO_2 (396 ± 3.0 µatm) did not vary greatly during the cruise. The seawater pCO_2 varied greatly during the cruise and maximum concentrations were observed in latitudes north of 40°N. At subarctic latitudes north of 38°N mean seawater pCO2 was 379 ± 39 µatm. The current axis mean pCO_2 was 337 ± 11 µatm. South of the axis mean pCO_2 was 322 ± 6.0 µatm. The ΔpCO_2 indicates the direction of gas diffusion. The Kuroshio Extension is a net drawdown of atmospheric CO_2. The mean $\Delta pCO_{2\ (sw\text{-}atm)}$ at latitudes between 30°N and 41°N was -52 ± 31 µatm. The large standard deviation is due to the small ΔpCO_2 in the axis of the Kuroshio Extension and at the northern latitudes (39°N to 41°N). At the axis mean ΔpCO_2 was -57 ± 11 µatm. In the subarctic region north of 38°N mean ΔpCO_2 was -18 ± 38 µatm. North of 40°N ΔpCO_2 was positive, indicating outgassing. The region south of the current axis (30°N to 34°N) had the greatest mean ΔpCO_2 (-73 ± 2.5 µatm).

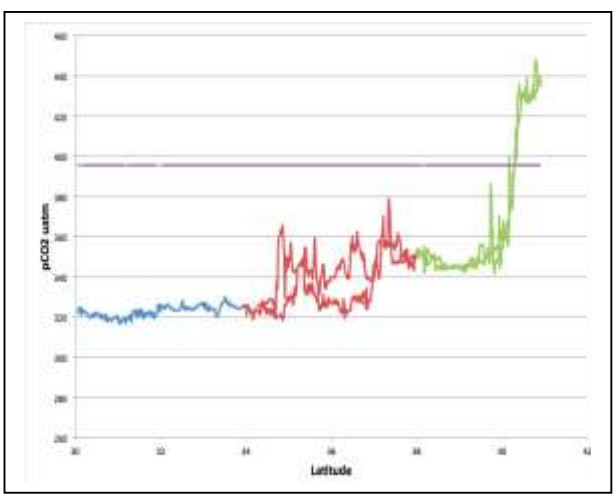

Fig. 4. Atmospheric and seawater pCO_2. The seawater pCO_2 is segmented into three regions: Kuroshio Extension south of the current axis (blue), the current axis (red) and the subarctic boundary (green). Mean atmospheric pCO_2 is represented in purple.

Wind speeds also varied greatly during the cruise (Fig. 5). Storm events generated winds to a maximum of 23 m s^{-1}. Mean wind speed during the entire cruise was 9.7 ± 4.8 m s^{-1}. The strongest winds were observed while transiting through the Kuroshio Extension axis (12 ± 5.8 m s^{-1}) however the axis is not defined by the presence of strong winds. The strong wind events observed during the cruise were by coincidence, which caused the large influx of CO_2 into the region (Fig. 6).

The rate of air-sea CO_2 exchange across latitudes 30°N to 41°N is a net sink of atmospheric CO_2 with a mean flux of CO_2 was -11.6 ± 10 mmol CO_2 m^{-2} d^{-1}. The mean rate of air-sea CO_2 exchange in the region 30°N to 38°N was -13.9 ± 10 mmol CO_2 m^{-2} d^{-1}. The axis of the Kuroshio Extension had the greatest the mean flux of CO_2 was -18.0 ± 11 mmol CO_2 m^{-2} d^{-1} (Fig. 6). Much like the wind speed at the current axis, high uptake was observed, suggesting wind speed is the primary influence on the air-sea flux. If the CO_2 flux were controlled by ΔpCO_2, then I would expect the axis to have a high CO_2 influx because strong geostrophic advection would decrease DIC concentrations (Ayers and Lozier, 2012). The mean rate of air-sea CO_2 exchange in the subarctic boundary (38°N to 41°N) was -5.8 ± 8.0 mmol CO_2 m^{-2} d^{-1}. The efflux of CO_2 at 40°N is surprising because the wintertime pCO_2 is controlled by SST (Inoue, 2002). Upwelling in the Western North Pacific (Qiu, 2001) may cause surface pCO_2 to increase and it is possible advection of high pCO_2 (Ayers and Lozier, 2012) from the Western subarctic gyre into the Kuroshio-Oyashio boundary caused the observed pCO_2 trends. While the direction of the CO_2 flux in the subarctic boundary was controlled by ΔpCO_2 the magnitude of efflux was controlled by the wind speed.

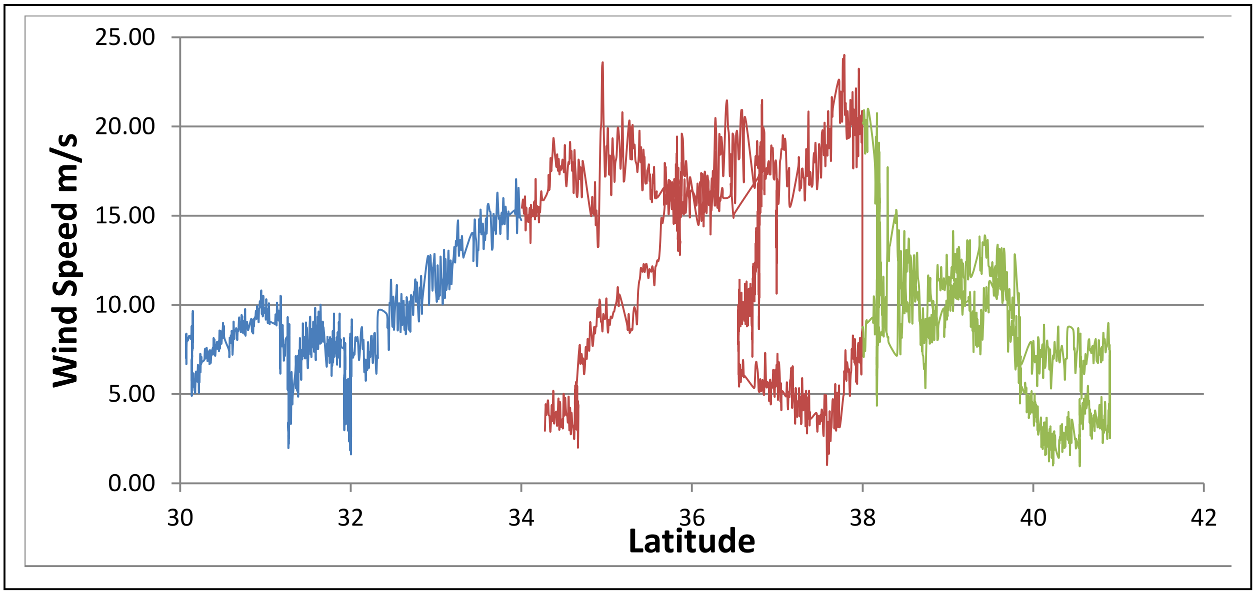

Fig. 5. Observed wind speed from the ship's MET system reported in m s^{-1}. The blue region indicates the Kuroshio Extension south of the current axis. The red region indicates the current axis and the green region indicates the northern boundary of the Kuroshio Extension. Differences in wind speed at like latitudes is due to differences during northward and southward transects.

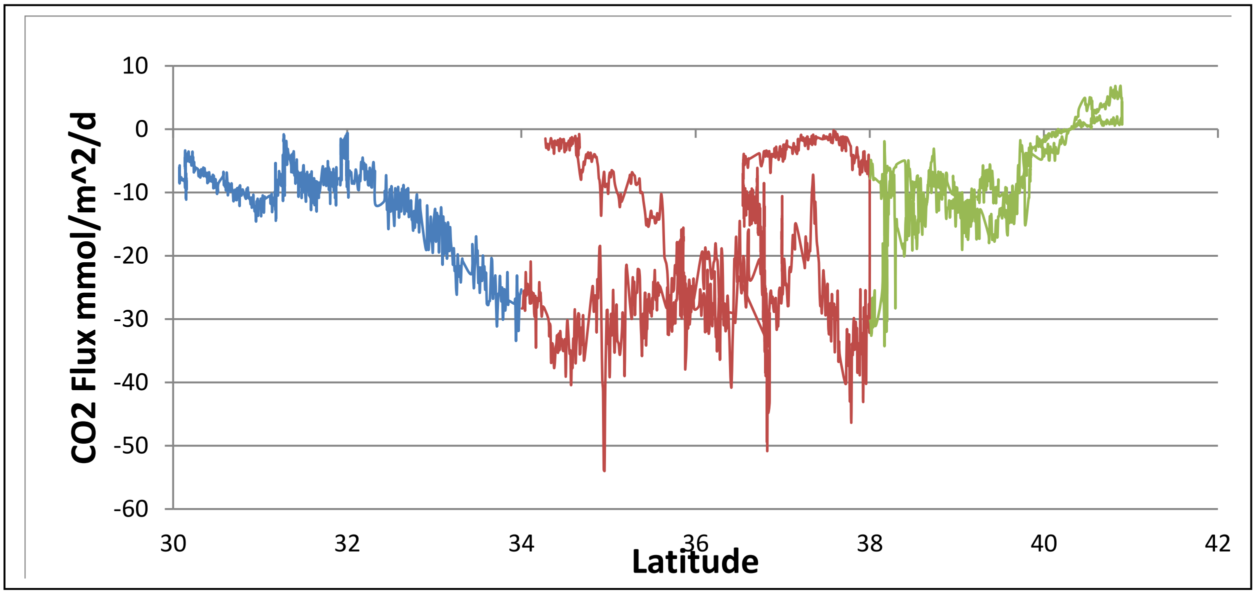

Fig. 6. CO_2 flux between 30°N and 41°N. The blue region indicates the Kuroshio Extension south of the current axis. The red region indicates the current axis and the green region indicates the northern boundary of the Kuroshio Extension. The negative flux values indicates influx of gas into the surface water while positive flux values indicate outgassing.

DISCUSSION & CONCLUSION

Controls on CO_2 flux

The axis of the Kuroshio Extension had the greatest mean ΔpCO_2 (-57 ± 11 μatm) and mean wind speed (12 ± 5.8 m s^{-1}). This led to a greater mean flux (-18 ± 11 mmol m^2 d^{-1}) than any other region of the cruise. While the large ΔpCO_2 concentrations were observed, its relationship to the CO_2 flux was not strongly correlated (R^2=0.15). The wind speeds appear to have a stronger relationship to the CO_2 flux (R^2=0.90) (Fig. 7). The proximity of the Kuroshio Extension axis to the western North Pacific, where annual winter storms are generated, increases the presence of strong wind events. The axis is also a region of a high SSH gradient due to convergence of cold fresher waters from the subarctic and warm saline waters from the subtropics (Jayne, 2009). The current axis is characterized by the strong geostrophic flow therefore lateral advection depletes surface water of DIC, therefore decreasing the pCO_2 (Ayers and Lozier, 2012). One would expect the relationship of ΔpCO_2 to the CO_2 flux to be strong however high ΔpCO_2 in the Kuroshio axis was not observed.

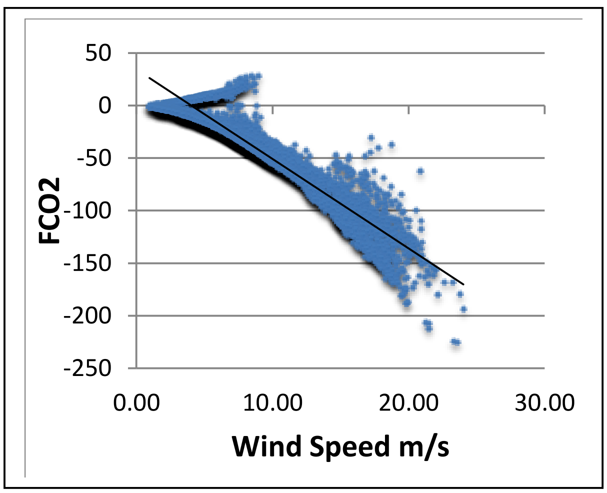

Fig 7. Linear regressions of CO_2 flux vs. wind speed, R^2=0.90. CO_2 flux is recorded in mmol m^{-2} d^{-1}.

Regional and Global Estimates

It is well known the North Pacific is a strong sink of atmospheric carbon however I wanted to know the role of the Kuroshio has in the North Pacific budget. The Kuroshio Extension is a net sink of atmospheric CO_2 at latitudes between 30°N and 40°N. Based on KEO data from 2009 (Fig. 8), the atmospheric pCO_2 concentration exceeds the seawater pCO_2 concentrations for approximately 9 months of the year (Fig. 8). Integrating the ΔpCO_2 observed at KEO during 2009 and dividing by the mean ΔpCO_2 observed during the month of February gives the number of months the Kuroshio Extension waters are undersaturated by the amount measured in February:

5. $(\int \Delta pCO_{2\_KEO} * dt)/\Delta pCO_{2\_Feb}$ = months of pCO_2 undersaturation

In this estimate I assume the Kuroshio Extension ΔpCO_2 is positive during the remaining months of the year. With a measured mean ΔpCO_2 of -52 ± 31 μatm and a 12 month integration of ΔpCO_2 at KEO of -302 ± 50 μatm, I calculate 5.8 months of understauration per year. This is approximately 3 months less than the observed 9 months of undersaturation at KEO. Using the measured mean flux -11.6 ± 10 mmol m^{-2} d^{-1}, I estimate the annual uptake of CO_2 in the Kuroshio Extension:

6. (mean CO_2 flux)$_{obs}$ * (days per year undersaturated) = moles Carbon m^{-2} yr^{-1}

From this I estimate an annual net flux of -2.0 mol CO_2 m^{-2} yr^{-1}. This is slightly lower than the regional uptake (-3 to -4 mol CO_2 m^{-2} yr^{-1}) calculated by Takahashi et al. (2002). This may be due to underestimations of the meridional extension of the Kuroshio. The observed rates were made between 30°N and 40°N however, regional ΔpCO_2 estimates (Takahashi et. al 2009) suggest the strong uptake of CO_2 extends to approximately 25°N.

To determine the amount of CO_2 taken up in the region, regional estimates of the meridional and longitudinal area of the Kuroshio Extension is required. Takahashi et al. (2009) estimated the broad meridional band of high net annual CO_2 in the Kuroshio extended from 140°E to 160°W. If I use the meridional distribution from 30°N to 40N, this is a cross sectional area of 5950500 km^2. Based on this area, and the molecular weight of carbon (12.01 g mol^{-1}) I estimate the Kuroshio

Extension has a net annual uptake of -0.14 Pg C yr^{-1}. Despite the underestimation of the

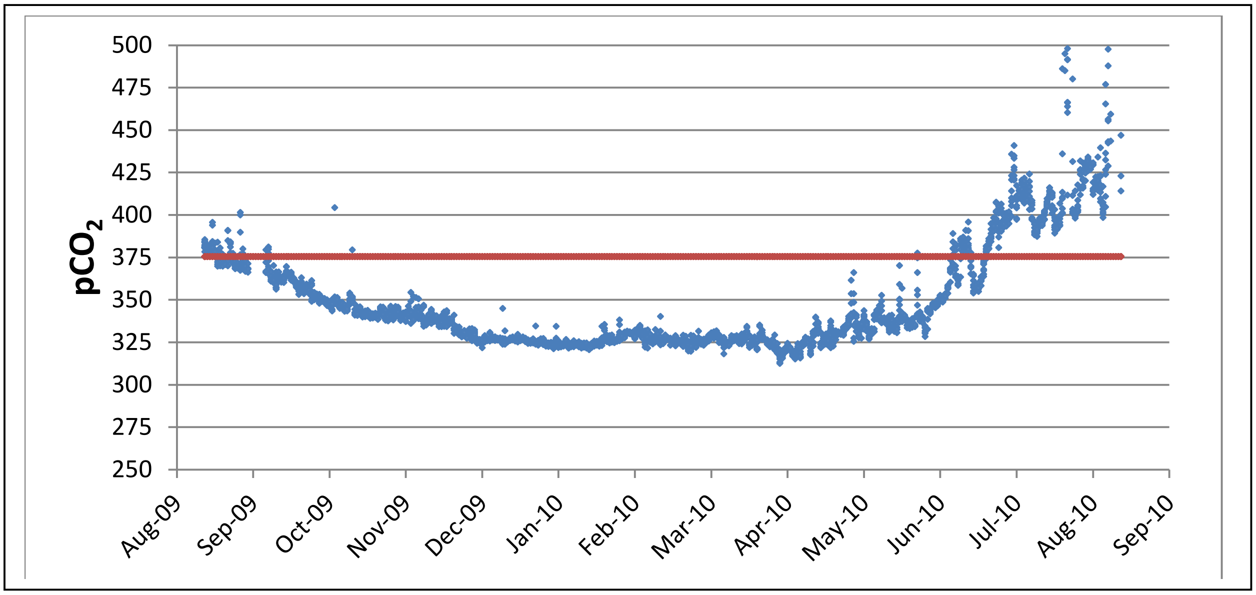

Fig. 8. Annual atmospheric (red) and seawater (blue) pCO_2 (μatm) at KEO between August 2009 and September 2010. Atmospheric pCO_2 is averaged to 375 μatm. Data provided by NOAA-Pacific Marine Environment Laboratory, Kuroshio Extension Observatory Seattle, Washington website: http://www.pmel.noaa.gov/keo/.

Kuroshio's meridional extent, the Kuroshio greatly influences the North Pacific's net annual uptake of carbon. Takahashi et al. (2002) estimated the North Pacific (14°N to 50°N) has a net annual flux of -0.64 Pg C yr^{-1}. Thus the Kuroshio Extension is responsible for 22% of the regional net annual uptake. Considering the estimated area of the Kuroshio compared to the total area of the North Pacific (approx. 3.0x10^{7} km^{2}) (Takahashi et al., 2009) the Kuroshio Extension draws down more carbon per square kilometer (-2.0 mol C m^{2} yr^{-1}) than all other regions of the North Pacific (1.4 mol C m^{2} yr^{-1}). Estimations of CO_2 flux in area of the Kuroshio Extension is important to quantify because current estimates of regional flux based on KEO data cannot account for the spatial variability. The 2009 mean ΔpCO_2 during the month of February at KEO was -57 ± 4.2 μatm. This is similar to the observed meridional mean from 30°N to 41°N (-52 ± 31 μatm). While these values are agreeable the meridional variability is not accounted for when estimating the carbon drawdown of the region based on KEO data. The SST and SSH anomalies vary throughout the extension and affects the seawater pCO_2 through surface water heat transport (Qiu, 2002; Stephens 1995). Recently Juranek et al. (2012) determined the advection of DIC to not only contribute to the CO_2 flux but also contribute to the location of influx. Understanding the effect physical processes and its variability in the Kuroshio extension will further improve estimates of the air-sea CO_2 flux.

Large currents driven by strong geostrophic flow such as the Kuroshio axis play a significant role in the uptake of atmospheric carbon. A changing climate may decrease this strong flow as SSH gradients decrease with sea surface warming. If regions such as the Kuroshio decrease the lateral advection of high DIC surface water, then the rate of carbon uptake will decrease. Greater spatial measurements and further research, such as this study, of the longitudinal extent of the Kuroshio Extension will lead to more accurate estimations of the regions global impact on carbon uptake.

ACKNOWLEDGEMENTS

I would like to thank my parents for providing me the resources to pursue my studies at the University of Washington. Steve Emerson, Steve Riser and the Ocean 444 TA's for giving me the opportunity to participate in the Japan senior thesis cruise as well as their guidance in my studies. A special thank you to NOAA PMEL for allowing me to use their pCO_2 data for this study. Finally, thank you to the School of Oceanography senior class for their insight during this project.

REFERENCE LIST

Ayers, J., and Lozier, M. 2012, Unraveling dynamical controls on the North Pacific carbon sink. J. Geophys. Res. 117: C01017, doi:10.1029/2011JC007368.

Cheney, R E. 1977. Synoptic Observations of the Oceanic Frontal System East of Japan. Journal of Geophysical Research. 82: No. 34

Cronin, M., Meinig, C., Sabine, C., Ichikawa, H., Tomita, H. 2008. Surface Mooring Network in the Kuroshio Extension. IEEE Systems Journal. 2: 3

Emerson, S., Hedges, J. Chemical Oceanography and the Marine Carbon Cycle. Cambridge University Press, 2008

Feely, R., Wanninkhof, R., Milburn, H., Cosca, C., Stapp, M., Murphy, P. A new automated underway system for making high precision pCO_2 measurements onboard research ships. Analytica Chimica Acta. 377. 185-191

Inoue, H., Ishii, M., Matsueda, H., Kawano, T., Murata, A., Takasugi, Y. 2003. Distribution of the partial pressure of CO_2 in surface water (pCO_2^w) between Japan and Hawaiian Islands: pCO_2^w – SST relationship in the winter and summer. Tellus. 55B: 456-465

Juranek, L., Quay, P., Feely, R., Lockwood, D., Karl, D., Church, M. 2012. Biological Production in the NE Pacific and its influence on air-sea CO_2 flux: Evidence from dissolved oxygen isotopes and O_2/Ar. Journal of Geophysical Research. 117: C05022, doi:10.1029/2011JC007450, 2012

Murata, A., Kaneko, I., Nemoto, K., Fushimi, K., Hirota, M. 1998. Spatial and temporal variations of surface seawater f_{CO2} in the Kuroshio off Japan. Marine Chemistry. 59: 189-200.

Nightingale, P., Malin, G., Law, C., Watson, A., Liss, P., Liddicoat, M., Boutin, J., Upstill-Goddard, R. 2000. In situ evaluation of air-sea gas exchange parameterizations using novel conservative and volatile tracers. Global Biogeochemical Cycles. 14: 1. 373-387

Qiu, B. 2001. Kuroshio and Oyashio Currents. AcademicPress, doi:10.1006/rwos.2001.0350

Qiu, B. 2002. The Kuroshio Extension System: Its Large-Scale Variability and Role in the Midlatitude Ocean-Atmosphere Interaction. Journal of Oceanography. 58. 57-75

Sarmiento, J. F and Gruber, N. 2002. Sinks for Anthropogenic Carbon. Physics Today. August 2002.

Stephens, M., Samuels, G., Olson, D., Fine, R. 1995. Sea-air flux of CO_2 in the North Pacific using shipboard and satellite data. Journal of Geophysical Research. 100: C7.

Takahashi, T., Sutherland, S., Sweeny, C., Poisson, A., Metzl, N., Tilbrook, B., Bates, N., Wanninkhof, R., Feely, R., Sabine, C., Olafsson, J., Nojiri, Y. 2002. Global sea- air CO_2 flux based on climatological surface ocean pCO_2, and seasonal biological and temperature effects. Deep-Sea Research II. 49: 1601-1622

Takahashi, T. and others. 2009. Climatological mean and decadal change in surface ocean pCO_2, and sea-air CO_2 flux over the global oceans. Deep-Sea Research II. 56: 554-577

Wanninkohf, R. 1992. Relationship Between Wind Speed and Gas Exchange Over the Ocean. Journal of Geophysical Research. 97: C5. 7373-7382

Weiss, R. 1974. Carbon dioxide in water and seawater: the solubility of a non-ideal gas. Marine Chemistry 2:203-215, http://dx.doi.org/10.1016/0304-4203(74)90015-2